



Journal of  
**Software  
Engineering**

ISSN 1819-4311



Academic  
Journals Inc.

[www.academicjournals.com](http://www.academicjournals.com)

## Evaluation on Available Transfer Capability of Power System Considering Wind Speeds Correlation

<sup>1</sup>Limei Zhang, <sup>1</sup>Yongfu Liu and <sup>2,3</sup>Jun Wang

<sup>1</sup>College of Information Science and Technology, Agricultural University of Hebei, Baoding, 071001, China

<sup>2</sup>School of Electrical Engineering and Automation, Harbin Institute of Technology, Harbin, 150001, China

<sup>3</sup>College of Information and Electric Engineering, Shenyang Agricultural University, Shenyang, 110866, China

*Corresponding Author: Jun Wang, School of Electrical Engineering and Automation, Harbin Institute of Technology, Harbin, 150001, China*

### ABSTRACT

The output power of wind turbines or wind farms depends on wind speeds, which may have certain correlation in one region or even in different regions. When the wind speeds correlation is ignored, it will have a significant influence on Available Transfer Capability (ATC) of power system with wind farms. This study established a random variables simulation method considering wind speeds correlation to more accurately evaluate ATC. The proposed methods are concerned with rank correlation coefficient, Copula theory and Monte Carlo Simulation (MCS), which are simple and easy to implement. In addition, the evaluation models for ATC were built on based of Optimal Power Flow (OPF) and Fast Voltage Stability Indices (FVSI) was considered as inequality constraints in order to guarantee the voltage stability of system. The modern interior point method was applied to solve the proposed models. Simulations are carried out on IEEE 118-bus system. The results show effectiveness and availability of the proposed method in evaluating on ATC of power system considering wind speeds correlation. The conclusion can provide a technical support for the ATC evaluation and decision-making as well as wind power forecast.

**Key words:** Voltage stability, wind power, correlation, available transfer capability, evaluation

### INTRODUCTION

With the rapid development of the wind power technology, wind farm sizes are becoming larger and larger day by day and consequently the proportion of wind electricity in power system will present the large-scale development trend (Usaola, 2010; Zhou *et al.*, 2010). A large scale of wind power access to power system, will inevitably have profound influences on power system due to the intermittency and uncertainty of wind energy (Chen *et al.*, 2011; Falaghi *et al.*, 2012). Therefore, evaluating and forecasting the impacts of high penetration of wind power are becoming a hot topic of research on power system evaluation fields.

As one of many significant influences, researches for impact on ATC of wind power have been discussed in order to ensure operation security of electric power and improve scientific decision. ATC of wind farm incorporated system were studied (Wang and Ding, 2010; Usaola, 2010; Zhou *et al.*, 2010) and a good evaluation method was established under considering uncertainty of renewable system (Wang and Ding, 2010; Falaghi *et al.*, 2012). But they don't take into account the

correlation between different random variables such as wind speed or wind power, load, etc. However, the wind speeds which determine the output power of wind turbine, have a certain correlation in certain areas or different regions. And there may be a certain dependencies between the similar loads. If the correlation between random variables is ignored, it can make some calculation results distort. When the error results are applied in the planning, operation or analysis fields of power system, it has direct effect to the system security stability and economy.

With the integration of large-scale wind power, power system will present more uncertainties. For these uncertainties, Monte Carlo method is usually employed in many references (Falaghi *et al.*, 2012; Wang and Ding, 2010) due to its simplicity and availability for the random problem. However, its application in some researches also did not consider the dependent relationships between random variables (Morales *et al.*, 2010; Yu *et al.*, 2009). Even if dependency was presented, it didn't overcome the shortcoming of computation-intensive, time-consuming and calculation-precision of Monte Carlo method. In the study of Wang and Ding (2010), a linear correlation coefficient was employed to approximately describe the dependency but it still need to consume a large amount of computing time. In the related random variable simulation (Usaola, 2010; Morales *et al.*, 2010) applied gram-Schmidt orthogonalization, Cornish-Fisher unfolds, etc. but models are complex and the time-consuming. The simulated annealing algorithm and genetic algorithm are employed, respectively to the sampling of random variable in the study of Vorechovsky and Novak (2009) and Liefvendahl and Stocki (2006) but the calculation-precision is still not good enough. Kalagnanam and Diwekar (1997) proposed Hamersley sampling method but it needs to deal with the reverse transformation of a large number of prime's roots.

Currently, existing researches are mainly focused on the assessment of ATC under uncertainty. In view of the difficulty and complexity in dealing with uncertainties, some researches adopted DC power flow model to reduce the amount of calculation, shortening computing time in the conditions of guaranteeing the accuracy (Li *et al.*, 2008; Rodrigues and da Silva, 2007) but this causes the voltage stability problem which should be considered seriously when a power system is connected with wind farms. And when ignoring the voltage stability, the evaluation effect of ATC will lead to serious errors. Usaola (2010), Zhou *et al.* (2010) and Wang and Ding (2010) adopted AC power flow model and incorporated the voltage stability by using the node voltage amplitude constraints. However, Yokoyama *et al.* (1991) and Paensuwan *et al.* (2010) indicated the shortcoming of the node voltage amplitude constraints. That is, it is not fully effective in avoiding voltage instability. For example, voltage instability or voltage sag will happen when reactive power support is insufficient. Under this environment, if corrective measures aren't implemented, it may eventually lead to voltage collapse.

This study established a random variables simulation method considering wind speeds correlation to more accurately evaluate ATC. The models for evaluation of ATC are presented on based on the AC power flow and adding FVSI inequality constraints to guarantee the voltage stability of system. Modern interior point method was proposed to solve optimal power flow problem.

## **MATERIALS AND METHODS**

**Description for evaluation model of ATC considering voltage stability:** According to the research content and the employed algorithms, the models focus on the following study: ATC computing models, voltage stability indices and wind power.

**Description for ATC computing models:** Load factor  $\lambda$  which is defined as the ratio of actual generating capacity and maximum generating capacity, is applied to measure the growth degree of load. The value of  $\lambda$  is zero at the beginning of load and increase with the rise of active power at each node, which corresponds to the transmission of electricity. Therefore, ATC can be obtained at the maximum of  $\lambda$ . The calculation of ATC is shown in Eq. 1:

$$P_{ATC} = \sum_{i \in \Omega} P_{Di} - \sum_{i \in \Omega} P_{Di}^0 - P_{CBM} \quad (1)$$

where,  $\Omega$  is the node set.  $P_{ATC}$  is the available transfer capability of power grid.  $P_{CBM}$  is Capacity Benefit Margin (CBM) which is 5% of the maximum transmission capacity in this study,  $P_{Di}^0$  is initial load power at  $i$  node.  $P_{Di}$  is load power at the maximum of  $\lambda$  which is given in Eq. 2:

$$P_{Di} = P_{Di}^0 + b_{Pi} \times \lambda_{max} \quad (2)$$

where,  $b_{Pi}$  is the growth proportion of active load at  $i$  node, that is the ratio of existing load and the initial load and  $\lambda_{max}$  is the maximum of  $\lambda$ .

In this study,  $\lambda_{max}$  is obtained by solving optimal power flow. The optimization model is as following:

$$\begin{cases} \text{Max } \lambda \\ \text{s.t. } f(x, \lambda) = 0 \\ h(x) \leq 0 \end{cases} \quad (3)$$

where,  $f(x, \lambda)$  is AC power flow equations. The inequality equations  $h(x)$  consider generating capacity constraints, voltage stability constraints, line thermal stability constraints, etc.

**Description for voltage stability index:** In existing researches, there are several types of voltage stability index. Here Fast Voltage Stability Index (FVSI), is selected as voltage stability constraints, whose specific theoretical derivation process can be founded in the study of Musirin and Rahman (2002). Its formulation is as follows:

$$FVSI_{ij} = \frac{4Z_{ij}^2 Q_j}{U_i^2 X_{ij}} = \frac{4Z_{ij}^2 (B_{ij}(e_j^2 + f_j^2 - e_i e_j - f_i f_j) - G_{ij}(e_j f_i - e_i f_j))}{X_{ij}(e_i^2 + f_i^2)} \quad (4)$$

where  $i, j$  are the first and end node numbers of line.  $Z_{ij}$  and  $X_{ij}$  are the line impedance and reactance.  $U_i$  is voltage amplitude at  $i$  node.  $Q_j$  is reactive power at  $j$  node.

The greater the FVSI value is, the worse the voltage stability is. When FVSI is close to 1, the voltage stability is the worst. Therefore, the voltage stability should satisfy Eq. 5:

$$FVSI_{ij} \leq 1 \quad (5)$$

**Description for the wind power:** The power of wind power depends on the wind speed which is sensitive to the natural factors, season variation and geographic environment and etc. So, wind

speed distribution varies substantially from place to place. Generally, two-parameter Weibull distribution is a common and effective technique in describing wind uncertainty (Li, 2006). Its probability density function is shown in Eq. 6:

$$\varphi(v) = \frac{k}{c} \left(\frac{v}{c}\right)^{k-1} \exp\left[-\left(\frac{v}{c}\right)^k\right] \tag{6}$$

where,  $k$ ,  $c$  is the shape parameter and the scale parameter.

Integrated with the actual working condition of WTGs, the power of wind power is expressed by the following equation:

$$P_w = \begin{cases} \frac{P_r(v - V_i)}{(V_r - V_i)} & V_i \leq v < V_r \\ P_r & V_r \leq v \leq V_o \\ 0 & v > V_o \text{ or } v < V_i \end{cases} \tag{7}$$

where,  $P_r$  and  $P_w$  are the rated power and active power output variables (MW) of WTGs, respectively.  $V_i$ ,  $V_r$  and  $V_o$  is orderly the cut-in wind speed, rated wind speed and cut-out wind speed ( $m \text{ sec}^{-1}$ ) and  $v$  is the wind speed variable.

**Simulation method of correlation wind speed:** The simulation method of correlation wind speed is carried out according to rank correlation coefficient, Copula Theory and Monte Carlo.

**Rank correlation coefficient:** The correlation coefficient is usually considered in dealing with the correlative problems between random variables. As the known dependence measure, the product moment (linear) correlation  $\rho$  or named as Pearson correlation is often used in this setting due to the characteristics of accurate measurement for the degree of linear dependencies between random variables and is invariant to linear transformations. In addition, it still describes the nonlinear dependencies between normal distribution variables. So, Pearson correlation can be used to solve the load obeying normal distribution (Vetterling *et al.*, 1992).

Assume that  $L$  is a load vector,  $Z_s$  is standard normal vector,  $\mu_L$ ,  $\sigma_L$  and  $\rho_L$  are mean vector, standard deviation vector and product moment correlation coefficient matrix of  $L$ . Then:

$$L = \sigma_L^T \cdot Z_s + \mu_L \tag{8}$$

Thus load vector  $L$  are set immediately when  $Z_s$  is specified. And  $Z_s$  follows from Cholesky decomposition, which can be shown as following:

$$Z_s = \begin{bmatrix} z_{s1} \\ z_{s2} \\ \vdots \\ z_{sN} \end{bmatrix} = C \times Z = \begin{bmatrix} c_{11} & & & \\ c_{21} & c_{22} & & \\ \vdots & & \ddots & \\ c_{N1} & c_{N2} & \cdots & c_{NN} \end{bmatrix} \begin{bmatrix} z_1 \\ z_2 \\ \vdots \\ z_N \end{bmatrix} \tag{9}$$

where,  $C$  is a lower triangular matrix from Cholesky decomposition.  $z_i = (i=1,2,\dots,N)$  is standard normal variable.

However, Pearson correlation  $\rho$  is affected by the marginal distributions and is not invariant to increasing transformations when it is applied in the actual domain of the random variables. To overcome these shortcomings, the rank correlation  $\rho_r$  (Spearman correlation) which is the product moment correlation of ranks, come forward according to cumulative distribution function. For example, the rank correlation of the random variables  $X$  and  $Y$  with cdf  $F_X$  and  $F_Y$  is defined as (Vetterling *et al.*, 1992):

$$\rho_s(X, Y) = \rho(F_X(X), F_Y(Y)) \tag{10}$$

From Eq. 10, for uniform variables, product moment correlation  $\rho$  and rank correlation  $\rho_s$  are the same but in general both of them are different. For the joint Normal distribution, the relationship between  $\rho$  and  $\rho_s$  is as following (Papaefthymiou and Kurowicka, 2009):

$$\rho(X, Y) = 2 \sin\left(\frac{\pi}{6} \rho_s(X, Y)\right) \tag{11}$$

For multivariate problems, rank correlation matrix  $\rho_m$  can be used to express all mutual rank correlations between the random variables. For example,  $\zeta_1, \zeta_2, \dots, \zeta_n$  are normal uncertain variables, then the rank correlation matrix  $\rho_m$  is:

$$\rho_m = \begin{bmatrix} \rho(\zeta_1, \zeta_1), \rho(\zeta_1, \zeta_2), \rho(\zeta_1, \zeta_3) \cdots \rho(\zeta_1, \zeta_n) \\ \rho(\zeta_2, \zeta_1), \rho(\zeta_2, \zeta_2), \rho(\zeta_2, \zeta_3) \cdots \rho(\zeta_2, \zeta_n) \\ \rho(\zeta_3, \zeta_1), \rho(\zeta_3, \zeta_2), \rho(\zeta_3, \zeta_3) \cdots \rho(\zeta_3, \zeta_n) \\ \vdots \\ \rho(\zeta_n, \zeta_1), \rho(\zeta_n, \zeta_2), \rho(\zeta_n, \zeta_3) \cdots \rho(\zeta_n, \zeta_n) \end{bmatrix}$$

**Copulas:** The copula, which is put forward by Sklar (1959), is actually a kind of function that joins or ‘couple’ one-dimensional marginal distributions in multivariate distribution functions. In other words, copulas are multivariate distribution functions whose one-dimensional marginal is uniform on the interval  $[0, 1]$ . The marginal distribution describes the distribution of the variable while copula function describes the correlation between variables. Nelsen (2006) defined Copula function as:

The random variables  $X_1, X_2, \dots, X_N$  with cdf  $F_{X_1}(x_1), F_{X_2}(x_2), \dots, F_{X_N}(x_N)$ , are joined by copula  $C$ , if their joint distribution can be written:

$$F(x_1, x_2, \dots, x_N) = C(F_{X_1}(x_1), F_{X_2}(x_2), \dots, F_{X_N}(x_N)) \tag{12}$$

Compared with the traditional methods for dependence measures, copulas have many incomparable advantages such as flexibility in constructing multivariate distribution, simplicity in building models, invariance of consistency and correlation in dealing with nonlinear transformation, feasibility and practicality in solving nonlinear, asymmetric and tail dependence between variables. Therefore, it is introduced and borrowed in many literatures. So, far, there are

many known families of copulas like the Normal (Gaussian) copula, the Elliptical copulas, the Archimedean copulas, the Diagonal band copula, etc (Papaefthymiou and Kurowicka, 2009; Nelsen, 2006). According to the research contents, this study introduces detailedly the properties of the Normal copula.

The Normal/Gaussian copula is the copula that corresponds to the multivariate Normal distribution. The copula can be constructed from the multivariate Normal distribution using Eq. 12. For n-dimensional normal uncertain variables, the copula function can be expressed as:

$$C(u_1, u_2, \dots, u_N; R) = \Phi_p(\Phi^{-1}(u_1), \Phi^{-1}(u_2), \dots, \Phi^{-1}(u_N)) \quad (13)$$

where, R is product moment correlation matrix,  $\Phi$  is the multivariate Normal distribution function and  $\Phi^{-1}$  is the inverse of the standard Normal distribution.

Generally speaking, the cdf transformation can transfer all random variables of the problem to a uniform domain and the rank of random variables before and after the transformation is consistent, that is, the dependence of random variables is unchanged. Furthermore, the random variables in the field of uniform distribution can be further transformed back to their original distributions by the inverse-cdf transformation without any loss of information. But correct and reasonable copula function is crucial issue to carry out transformation between original distributions domain and uniform domain. Obviously, it is more convenient to investigate and model stochastic dependence in the uniform domain than in the actual domain but. Therefore, here the normal copula function shown in Eq. 13 is applied to solve the scheme design for measurement and sample test.

**Simulation method for wind speed based on normal copula function:** The following three tasks should be followed when extracting n-dimension random variables corresponding to rank correlation coefficient matrix  $R_s$  based on the normal Copula function:

- The random variable with standard normal distribution should be obtained according to the given rank correlation coefficient matrix  $R_s$
- The uniform distribution number  $U_m$  in interval [0, 1] with rank correlation coefficient matrix  $R_s$  are generated by using the random variable with standard normal distribution and the normal Copula function
- The random variable with marginal distribution  $W_m$  are obtained by the inverse of the cumulative distribution function which is shown in Eq. 14:

$$W_m = F_m^{-1}(U_m) \quad (14)$$

When applying the normal copula function to simulate the correlation wind speeds, the detailed flows are described as following:

**Step 1:** Integrated with the rank correlation coefficient matrix of wind speeds  $R_s$  given by wind power plant or wind turbine generator. Product moment correlation coefficient matrix R is calculated by Eq. 11

**Step 2:** N independent standard normal distribution sampling  $z_i (i = 1, 2, \dots, N)$  are realized by Monte Carlo simulation method

**Step 3:** By the Cholesky decomposition of R, lower triangular matrix  $C_R$  can be obtained. N dependent standard normal distribution random variables  $Y_w$ , whose product moment correlation coefficient matrix is R, are calculated by Eq. 15:

$$Y_w = \begin{bmatrix} Y_{w1} \\ Y_{w2} \\ \vdots \\ Y_{wn} \end{bmatrix} = C_R \times Z = \begin{bmatrix} c_{R11} & & & \\ c_{R12} & c_{R22} & & \\ \vdots & & \ddots & \\ c_{RN1} & c_{RN1} & \cdots & c_{RNN} \end{bmatrix} \begin{bmatrix} Z_1 \\ Z_2 \\ \vdots \\ Z_N \end{bmatrix} \quad (15)$$

**Step 4:** Based on the normal copula function, N uniform distribution random variables  $U_m$  in interval [0, 1] with rank correlation coefficient matrix  $R_s$  are generated by the transformation of  $Y_w$  and Eq. 13, that is:

$$U_m = \Phi_p = m = 1, 2, \dots, N \quad (16)$$

**Step 5:** The wind speed sampling with rank correlation coefficient matrix  $R_s$  is carried out by Eq. 14

**Calculation process for available transfer capability of power grid:** Combined with the aforementioned formulations and the sample method, the calculation process for available transfer capability of Power Grid mainly include generation of random samples for wind speed and load, determination of the parameter and the state of the systems, calculation of available transfer capability, evaluation and analysis of different probability index. Its detailed information is enunciated as follows:

- Step 1:** According to simulation method, the random samples for wind speed are generated by wind speed information such as Weibull distribution function, rank correlation coefficient matrix, the mean, standard deviation, etc
- Step 2:** The systematical parameters and states are given by determining equipment status corresponding to each sampling
- Step 3:** Based on Monte Carlo simulation, the available transfer capability corresponding to each sampling is obtained by Eq. 3. The specific calculation method can be founded in the method of Wei and Ding (2002)
- Step 4:** The evaluation and analysis of systematical ATC is implemented by computing probability index like the mean, standard deviation and risk degree of ATC. Here the risk degree is defined as the probability of ATC less than or equal to the specific ATC values required by power system. It can be shown in Eq. 17:

$$R_{\text{risk}}(ATC_T) = \frac{N_i(ATC_i \leq ATC_T)}{NS} \quad (17)$$

where, NS is the number of Monte Carlo simulations.  $ATC_T$  is the specific ATC values required by power system.  $N_i$  is the number of ATC less than or equal to  $ATC_T$ .



**RESULTS AND DISCUSSION**

**Test system and simulation parameters:** To demonstrate the proposed method and analyze the impact of wind speeds correlation on ATC of Power Grid, simulation is carried out on IEEE 118-bus system. Its topological structure and the branch, load parameters are founded in MATPOWER 4.1. Here the IEEE 118-bus system is divided into two zones: One for power generation, the other for reception energy. The schematic of partitions is shown in Fig. 1. This study assumed that there are four wind power plants in the zone for reception energy which are respectively set up at the node 44, 60, 83 and 83. The parameters for wind power plant are shown in Table 1.

**Validity analysis for interior-point method:** Interior-point method is employed to solve optimization with nonlinear equality and inequality constraints. Considering with FVSI inequality constraint, the effectiveness and the adaptability of interior-point method are simulated and analyzed. Complement clearance are taken as performance index of reflecting effectiveness of the interior-point method. The convergence criterion of algorithm is whether complement clearance can attain the required accuracy or not. Figure 2 shows the iterative curves of algorithm with or without FVSI constraint. From Fig. 2, the iteratives iterates with FVSI constraint are slightly more than that without FVSI constraint, that is, the former is 19 and the latter is 23. So, the algorithm has good robustness.

**Impact of wind speeds correlation on ATC:** Table 2 list mean and variance of ATC under different rank correlation coefficient of wind speeds. From Table 2, the mean of ATC is almost invariable under different correlation coefficient but the variance of ATC is continuously increasing

Table 1: Relevant parameters of wind farms

| Wind farms | No. of wind turbines | Rated power (MW) | Cut-in wind speed (m sec <sup>-1</sup> ) | Cut-out wind speed (m sec <sup>-1</sup> ) | K   | C   |
|------------|----------------------|------------------|--|---|-----|-----|
| 1          | 50                   | 1.7              | 4  | 15  | 1.5 | 6.5 |
| 2          | 50                   | 2.0              | 3  | 14  | 1.5 | 5.5 |
| 3          | 50                   | 1.5              | 4  | 15  | 1.5 | 6.5 |
| 4          | 50                   | 1.7              | 3  | 14  | 1.5 | 5.5 |

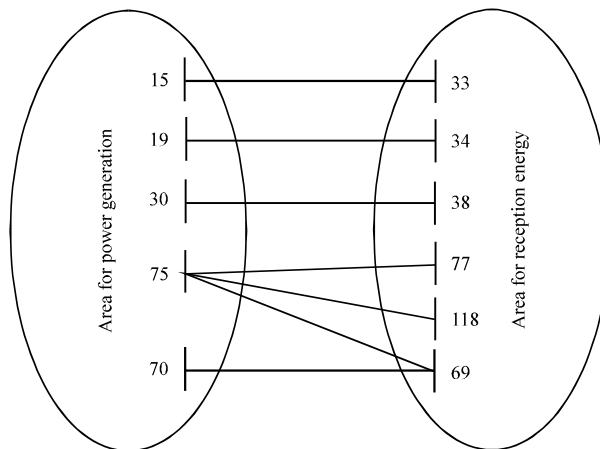


Fig. 1: Schematic of partitions for IEEE 118-bus system

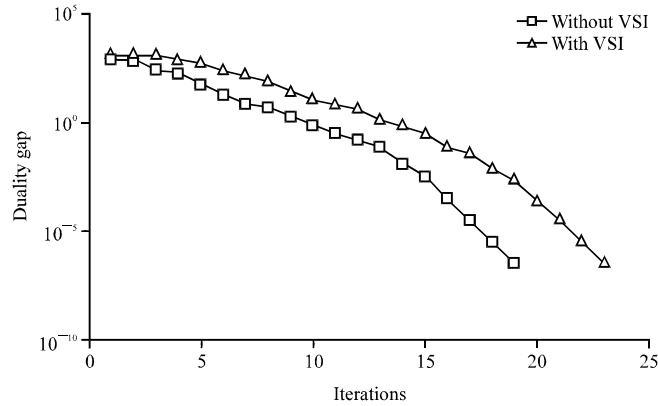


Fig. 2: ATC probability density for different correlation coefficient

Table 2: Mean value and variance of ATC under different correlation coefficient

|            | Rand correlation coefficient |        |        |        |        |        |
|------------|------------------------------|--------|--------|--------|--------|--------|
|            | 0.0                          | 0.2    | 0.4    | 0.6    | 0.8    | 1.0    |
| ATC index  | 0.0                          | 0.2    | 0.4    | 0.6    | 0.8    | 1.0    |
| Mean value | 1417.2                       | 1420.6 | 1417.5 | 1420.8 | 1417.4 | 1417.5 |
| Variance   | 3757.7                       | 5176.9 | 6958.5 | 8910.5 | 11500  | 15016  |

Table 3: ATC index for different risk level

|                         | ATC value for risk level (MW) |         |         |         |         |         |
|-------------------------|-------------------------------|---------|---------|---------|---------|---------|
|                         | 0.0                           | 0.2     | 0.4     | 0.6     | 0.8     | 1.0     |
| Correlation coefficient | 0.0                           | 0.2     | 0.4     | 0.6     | 0.8     | 1.0     |
| 0.0                     | 1333.86                       | 1363.59 | 1385.98 | 1402.98 | 1416.99 | 1435.90 |
| 0.2                     | 1319.52                       | 1358.62 | 1384.12 | 1407.17 | 1424.15 | 1442.65 |
| 0.4                     | 1301.43                       | 1337.86 | 1373.59 | 1395.74 | 1422.97 | 1446.71 |
| 0.6                     | 1280.43                       | 1327.57 | 1367.61 | 1402.67 | 1438.21 | 1462.09 |
| 0.8                     | 1254.06                       | 1307.50 | 1352.75 | 1392.26 | 1432.50 | 1465.14 |
| 1.0                     | 1218.30                       | 1284.85 | 1336.39 | 1383.28 | 1428.18 | 1475.29 |

with the increase of correlation coefficient. In other words, the bigger fluctuation of ATC will happen on the condition of the bigger correlation coefficient. These fluctuations show that bigger correlation coefficient may exert a bigger influence upon the accuracy of the probability evaluation of ATC.

Meanwhile, in order to understand how the rank correlation coefficient of wind speeds influence on the probability evaluation of ATC, the ATC indexes of different risk level are obtained by Eq. 17. The numerical results are listed in Table 3. Figure 3 and 4 show, ATC probability density and ATC cumulative distribution for different correlation coefficient.

Table 3, Fig. 3 and 4 all show that ATC probability distribution have quite a large difference under the same risk level but different correlation coefficient. Therefore, if the correlation of wind speed is ignored when carrying on evaluation of ATC, the assessment results could be incorrect or imprecision. It further shows that ATC is affected greatly by the wind speed correlation.

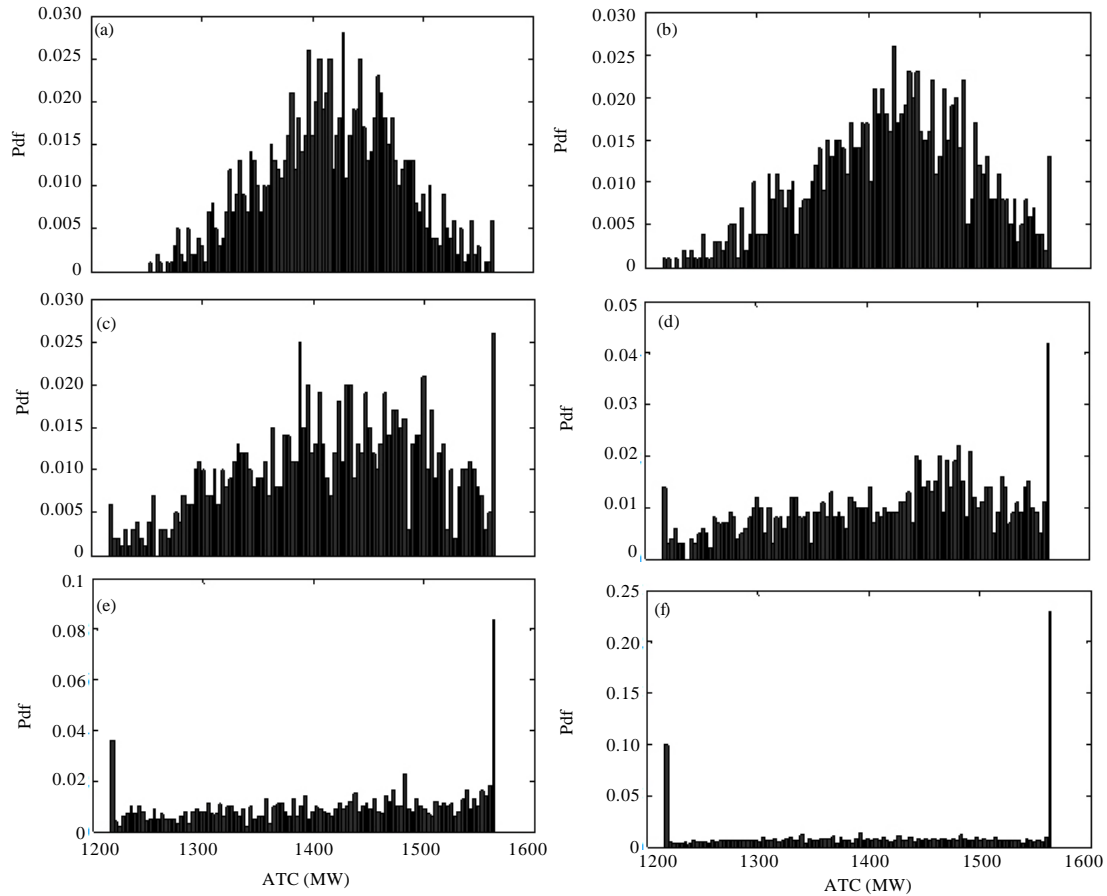


Fig. 3(a-f): ATC probability density for different correlation coefficient, ATC probability density for (a)  $\rho_s = 0$ , (b)  $\rho_s = 0.2$ , (c)  $\rho_s = 0.4$ , (d)  $\rho_s = 0.6$ , (e)  $\rho_s = 0.8$  and (f)  $\rho_s = 1.0$

From Fig. 3, it is founded that with the continuous increase of the correlation coefficient. The profiles of ATC probability density change gradually from high central portion and low on both sides to low central portion and high on both sides, namely the bigger the correlation coefficient, the greater the probability density of ATC boundary values.

From Fig. 4, ATC cumulative distributions under different correlation coefficient have almost the intersection point, where TAC is about 1412 MW and the risk level is about 46%. Below the intersection point, ATC under the same risk level decreases with the increase of correlation coefficient while above the intersection point, it is just the opposite. That is to say, ATC under the same risk level increase with the increase of correlation coefficient.

From Fig. 4, ATC cumulative distributions under different correlation coefficient have almost the intersection point, where TAC is about 1412 MW and the risk level is about 46%. Below the intersection point, ATC under the same risk level. Decrease with the increase of correlation coefficient while above the intersection point, it is just the opposite. That is to say, ATC under the same risk level increase with the increase of correlation coefficient.

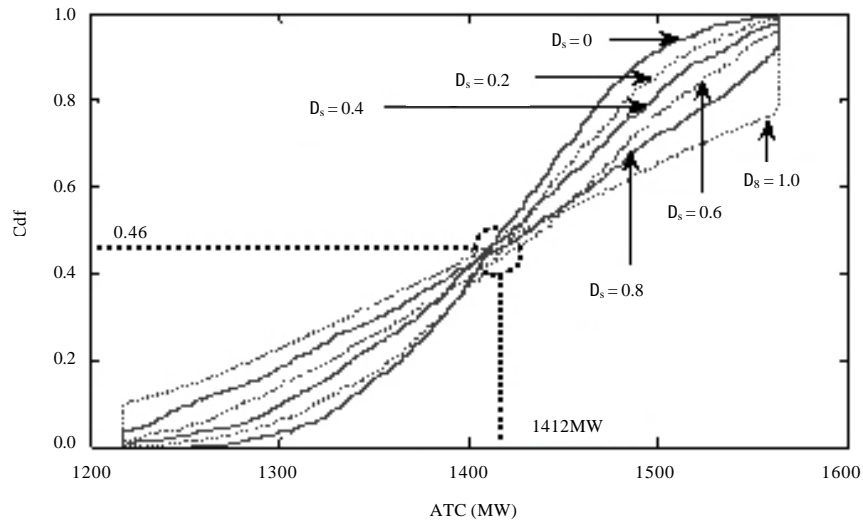


Fig. 4: ATC cumulative distribution under different correlation coefficient

## CONCLUSION

In order to more accurately evaluate ATC, this study investigated the effectiveness and the adaptability of interior-point method in solving optimization with nonlinear equality and inequality constraints including FVSI. The simulations demonstrate that the effectiveness and the adaptability of interior-point method are very high and the convergence criterion and convergence speed is satisfied for solving nonlinear optimization problem. In addition, the proposed random variables simulation methods considering wind speeds correlation based on rank correlation coefficient, Copula theory and Monte Carlo Simulation (MCS) are simple and easy to implement in modeling dependences between multi-variables of wind speed. The simulations on IEEE-118 demonstrate that the mean of ATC is almost invariable under different correlation coefficient but the variance of ATC is continuous increase with the increase of correlation coefficient. A large amount of simulations concluded that wind speeds correlations have a significant influence on ATC of wind farms grid-connected power system. Therefore, wind speeds correlations must not be ignored when calculating ATC. The presented method and the conclusion can provide a technical support for the ATC evaluation and decision-making as well as wind power forecast.

## ACKNOWLEDGMENTS

This study was supported by Hebei Science Research and Development Project of China (13215206), Liaoning Natural Science Foundation of China (201202191), Technology Foundation of Agricultural University of Hebei (LG20130801, LG20130804) and Hebei Engineer Research Center of Information Technology for Rural Area.

## REFERENCES

- Chen, Y., J. Wen and S. Cheng, 2011. Probabilistic power flow calculation considering the input variable. *Proc. Chin. Soc. Electr. Eng.*, 31: 80-87.
- Falaghi, H., M. Ramezani, C. Singh and M. Haghifam, 2012. Probabilistic assessment of TTC in power systems including wind power generation. *IEEE Syst. J.*, 6: 181-190.

- Kalagnanam, J.R. and U.M. Diwekar, 1997. An efficient sampling technique for off-line quality control. *Technometrics*, 39: 308-319.
- Li, G.Y., Y.J. Gao and M. Zhou, 2008. Sequential Monte Carlo simulation approach for assessment of available transfer capability. *Proc. CSEE*, 28: 74-79.
- Li, Y., 2006. *Power System Risk Assessment: Models, Methods and Applications*. Science Press, Beijing, China, ISBN: 9787030167316, Pages: 294.
- Liefvendahl, M. and R. Stocki, 2006. A study on algorithms for optimization of Latin hypercubes. *J. Stat. Plan. Inference*, 136: 3231-3247.
- Morales, J.M., L. Baringo, A.J. Conejo and R. Minguez, 2010. Probabilistic power flow with correlated wind sources. *IET Gener. Transm. Distrib.*, 4: 641-651.
- Musirin, I. and T.K.A. Rahman, 2002. Novel Fast Voltage Stability Index (FVSI) for voltage stability analysis in power transmission system. *Proceedings of the Student Conference on Research and Development*, July 16-17, 2002, Shah Alam, Malaysia, pp: 265-268.
- Nelsen, R.B., 2006. *An Introduction to Copulas*. Springer, New York, ISBN: 9780387986234, Pages: 216.
- Paensuwan, N., A.Yokoyama, S.C. Verma and N. Yoshiki, 2010. Voltage stability constrained risk-based TTC evaluation of a power system with large integration of renewable energy. *Proceedings of the International Conference on Power System Technology*, October 24-28, 2010, Hangzhou, China, pp: 1-6.
- Papaefthymiou, G. and D. Kurowicka, 2009. Using copulas for modeling stochastic dependence in power system uncertainty analysis. *IEEE Trans. Power Syst.*, 24: 40-49.
- Rodrigues, A.B. and M.G. da Silva, 2007. Probabilistic assessment of available transfer capability based on Monte Carlo method with sequential simulation. *IEEE Trans. Power Syst.*, 22: 484-492.
- Sklar, A., 1959. *Fonctions de Repartition A N Dimensions et Leurs Marges*. Vol. 8, Institute of Statistics, University of Paris, France, pp: 229-231.
- Usaola, J., 2010. Probabilistic load flow with correlated wind power injections. *Electr. Power Syst. Res.*, 80: 528-536.
- Vetterling, W.T., W.H. Press, S.A. Teukolsky and B.P. Flannery, 1992. *Numerical Recipes in C: The Art of Scientific Computing*, Volume 4. Cambridge University Press, New York, ISBN: 9780521437202, Pages: 994.
- Vorechovsky, M. and D. Novak, 2009. Correlation control in small-sample Monte Carlo type simulations I: A simulated annealing approach. *Probabilistic Eng. Mech.*, 24: 452-462.
- Wang, M. and M. Ding, 2010. Probabilistic calculation of total transfer capability including large-scale solar park. *Autom. Electr. Power Syst.*, 34: 31-35.
- Wei, H. and X. Ding, 2002. An algorithm for determining voltage stability critical point based on interior point theory. *Proc. Chin. Soc. Electr. Eng.*, 22: 27-31.
- Yokoyama, A., T. Kumano and Y. Sekine, 1991. Static voltage stability index using multiple load-flow solutions. *Electr. Eng. Jpn.*, 111: 69-79.
- Yu, H., C. Chung, K. Wong and J. Zhang, 2009. A probabilistic load flow calculation method with Latin hypercube sampling. *Autom. Electr. Power Syst.*, 33: 32-35.
- Zhou, M., R.J. Ran and G.Y. Li, 2010. Assessment on available transfer capability of wind farm incorporated system. *Proc. CSEE*, 30: 14-21.